ELSEVIER

Journal of Alloys and Compounds 446–447 (2007) 224–227

Journal of ALLOYS AND COMPOUNDS

www.elsevier.com/locate/jallcom

Application of pressure programmed absorption and desorption to characterize hydriding and dehydriding kinetics of $LaNi_5$ during activation

V. Fuster, F.J. Castro, G. Urretavizcaya *

Centro Atómico Bariloche (CNEA, CONICET) and Instituto Balseiro (UNC), Av. Bustillo 9500, R8402AGP S.C. de Bariloche, Argentina

Received 29 September 2006; received in revised form 2 February 2007; accepted 13 February 2007
Available online 17 February 2007

Abstract

Hydriding and dehydriding kinetics is an important aspect of the reaction of hydrogen with different hydride forming materials. In particular, it is a key factor in several applications of hydrogen from an energetic point of view. We present here the use of a recently developed technique to characterize hydrogen absorption and desorption kinetics: pressure programmed absorption and desorption (PPAD). The technique is based on an isothermal pressure-ramped measurement of the hydriding and dehydriding rate, and its principal advantages are the absence of an initial blind period, the short time required to complete an experimental run, and the possibility to automatically perform consecutive hydrogen absorption and desorption cycles. To illustrate this, we present the use of PPAD to follow the evolution of hydriding and dehydriding kinetics of $LaNi_5$ during the activation process. Additionally, we analyze the effect of using hydrogen with different purity levels.

Keywords: Hydrogen absorbing materials; Metal hydrides

1. Introduction

Nowadays, the advantages of hydrogen as an energy carrier or as a clean fuel are widely known. In the last decades great research and technological efforts have been made in the areas of hydrogen production, transportation, storage and use [1,2]. In particular, hydrogen storage in metallic hydrides has been extensively studied because it is the safest method for storage and transportation [1–4]. Several aspects of the formation and decomposition of metallic hydrides are important from scientific and technological points of view; some of them are material activation, hydrogen sorption kinetics, and gas impurities susceptibility [5].

We have recently developed a technique to characterize hydrogen absorption and desorption kinetics of hydride forming materials: pressure programmed absorption and desorption (PPAD) [6]. In a PPAD experiment we measure the isothermal rate of hydriding or dehydriding under a linear hydrogen-pressure ramp. The main advantages of this method are the absence of blind periods (a time interval during which data cannot be collected), the possibility to perform continuous hydriding and dehydriding cycles, and the requirement of small sample masses.

In this paper we study the evolution of hydrogen absorption and desorption kinetics by PPAD during the first activation cycles of $LaNi_5$. We also analyze the effects on the process of using hydrogen with different purities.

2. Experimental

High-purity commercial $LaNi_5$ (HyStor 205, Aldrich) was used as starting material. One-piece samples with masses of the order of 160 mg were placed into the reactor within a glove box under argon atmosphere. Prior to PPAD measurements, the system was purged three times with hydrogen at room temperature. High-purity hydrogen (99.99%) was used during the experimental runs. Two sets of experiments were carried out. In the first set, cycling was performed with extra-purified hydrogen obtained by circulation through oxygen and moisture traps. The sample cycled with this gas will be hereafter designated as "sample A". In the second set, the gas employed flowed straight from the supply. The sample will be hereafter designated as "sample B".

The experimental setup used to perform the PPAD measurements has been described elsewhere [6]. The measurements were performed at 48 °C with pressure increasing or decreasing linearly at 0.5 kPa/s. The pressure range

* Corresponding author. Tel.: +54 2944 445100; fax: +54 2944 445199.
E-mail address: urreta@cab.cnea.gov.ar (G. Urretavizcaya).

0925-8388/$ – see front matter © 2007 Elsevier B.V. All rights reserved.
doi:10.1016/j.jallcom.2007.02.064

was adjusted during the measurements in order to complete the hydriding and dehydriding processes.

3. Description of the technique

A typical absorption PPAD experiment starts at a hydrogen pressure well below the sample equilibrium pressure, and follows by hydriding the material isothermally, applying a linear hydrogen-pressure ramp. The rate of hydrogen entering the sample at each pressure is the main result of the experiment. A desorption experiment is performed similarly, but decreasing the pressure.

The equation that relates the hydrogen absorption or desorption rate with the experimentally measured quantities is obtained from the mass-balance equation of the system:

$$\frac{1}{2}\frac{\mathrm{d}n_\mathrm{H}}{\mathrm{d}t} + \frac{\mathrm{d}n_\mathrm{g}}{\mathrm{d}t} = \phi.$$

Here n_H represents the amount of H in the sample, n_g the quantity of hydrogen in gaseous form, and ϕ is the H_2 flow through the mass-flow controllers (positive, absorption; negative, desorption).

By using the ideal-gas law corrected by the compressibility factor, the rate of hydrogen absorbed or desorbed by the sample can be calculated as

$$\frac{\mathrm{d}n_\mathrm{H}}{\mathrm{d}t} = 2\phi - \frac{2VA}{RTZ^2}\frac{\mathrm{d}p}{\mathrm{d}t},$$

with V the volume of the reactor, p the pressure, T the temperature, R the universal gas constant and Z the compressibility factor, expressed as a function of pressure as

$$Z(p, T) = A + B(T)p.$$

A plot of the hydrogen absorption or desorption rates as a function of pressure typically shows a peak-shaped curve. This is a consequence of two opposite tendencies: an ascending rate due to the increase (absorption) or decrease (desorption) of pressure, and a descending rate due to the exhaustion of reactants as reaction proceeds.

4. Results and discussion

The most striking effects during $LaNi_5$ activation take place at the beginning of cycling. In Fig. 1 we present the first, second and sixty-second (full activation) absorption and desorption cycles of sample A. Absorption peaks, characterized by a positive rate, can be observed in the top half of the figure; desorption peaks, with negative rates, can be seen in the bottom half of the figure. In Fig. 2 we show the evolution of peak location with cycling. We describe peak location by the pressure where the maximum (absorption) or minimum (desorption) hydrogen flow occurs. As the cycling was performed at 48 °C, the corresponding equilibrium absorption and desorption pressures are 439 and 385 kPa, respectively [7]. We see that the first cycle absorption peak is located 1578 kPa above the equilibrium pressure, whereas the second cycle absorption peak is only 350 kPa above the equilibrium pressure, *i.e.* from the first to the second absorption cycle the absorption pressure diminishes

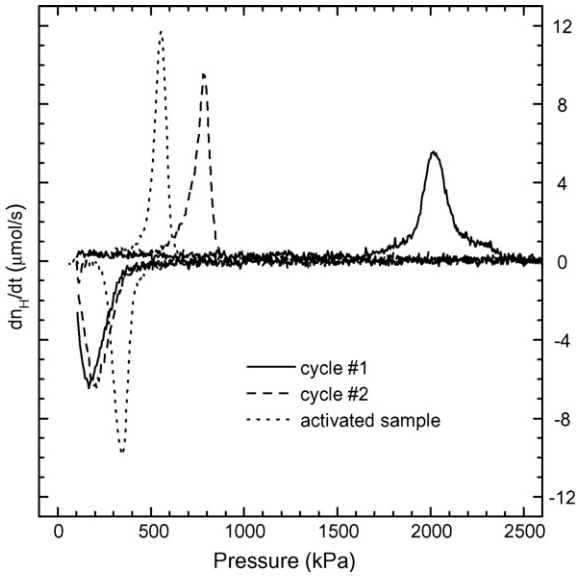

Fig. 1. First, second and sixty-second (activated sample) absorption/desorption cycles measured by PPAD on the $LaNi_5$ sample A at 48 °C and 0.5 kPa/s. Full line: first cycle; dashed line: second cycle; dotted line: sixty-second cycle.

approximately 1200 kPa. After the second cycle, the evolution consists of a gradual decrease of the absorption pressure down to 555 kPa, where the peak of the fully activated sample lies (see also Fig. 3A). The changes in the desorption peaks are not so drastic. From the first to the second desorption cycle, the peaks move up in pressure only 40 kPa, and the fully activated sample presents a desorption peak located at 345 kPa, only 177 kPa above the first desorption peak. This behavior, where absorption and desorption peaks move towards the equilibrium pressure as the system evolves, agrees with previously reported results [8], showing an important decrease of hysteresis in $LaNi_5$ isotherms

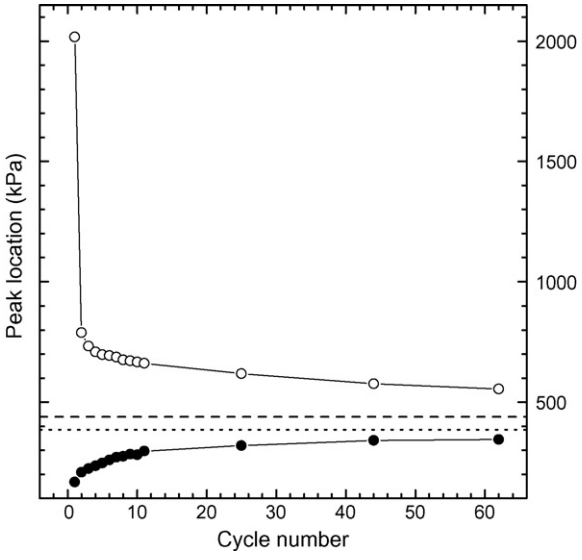

Fig. 2. Location of the maxima of the absorption and desorption peaks for sample A as a function of cycling. Open symbols: absorption maxima; full symbols: desorption maxima; dashed line: absorption equilibrium pressure at 48 °C; dotted line: desorption equilibrium pressure at 48 °C.

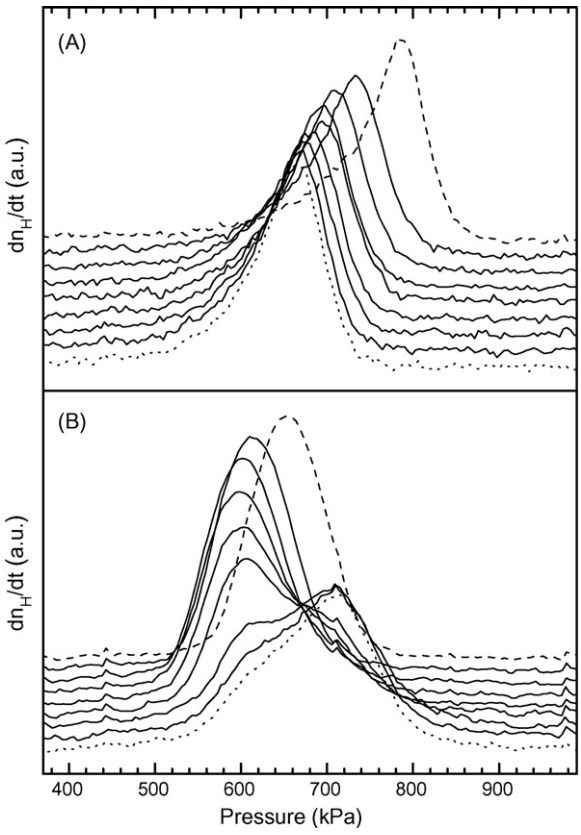

Fig. 3. First absorption curves of $LaNi_5$ at 48 °C and 0.5 kPa/s. (A) Sample A and (B) sample B. From top to bottom, cycles 2 (dashed line) to 10 (dotted line).

during the first hydriding and dehydriding cycles, mainly due to the diminution of the absorption pressure.

Also, in Fig. 1, we see that the shape of the absorption peaks changes substantially from the first to the second cycle. In the first cycle, we see a broad peak almost three times wider and of approximately half the height of the second cycle peak. This reduction in width and increase in height reflects an improvement in absorption kinetics as a consequence of the activation process. Desorption peak shape does not change considerably from the first to the second cycle. From the second cycle on, there are no important changes in absorption or desorption peak shape, only a sharpening reflecting the improvement in kinetics.

The capacity of the sample as a function of cycling can be determined by the area under the absorption and desorption peaks. The amount of hydrogen absorbed drops from 1.55 ± 0.08 wt% for the first cycle to 1.28 ± 0.08 wt% for the second one, while the amount of hydrogen desorbed in the first and second cycles is 1.3 ± 0.1 wt.%. After that, the capacity of the sample does not change within the experimental error. Up to now, we do not completely understand why the capacity falls from the first absorption to the first desorption (or second absorption). Possible explanations could be the reduction of nickel oxides originally present on the surface of the sample [9], or the formation of stable lanthanum hydrides [10].

The evolution during activation agrees with previously reported results [8,11,12]. As mentioned above, during the first

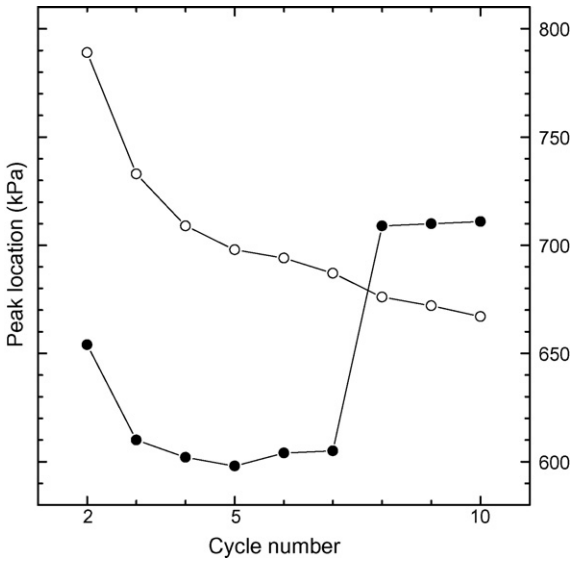

Fig. 4. Location of the maxima of the absorption peaks for samples A and B from the second to the tenth cycle. Open symbols: sample A and full symbols: sample B.

absorption and desorption cycles the activation consists of a reduction in the absorption pressure [8]. This evolution has been explained mainly as a consequence of the creation of planar defects and the decrepitation of the sample. Although the capacity fall observed between the first and second absorption cycles is not explicitly mentioned in the literature, a similar behavior seems to occur in Fig. 1 of Kisi et al. [8].

The first two cycles of sample B were similar to those of sample A. The first absorption cycle present a peak with a maximum at 1826 kPa, and the second cycle has its maximum at 654 kPa. The location of the maxima does not exactly match that of sample A (let us recall that we used one-piece samples, and as such the results are subject to coarse fluctuations caused by, for example, differences in the state of the surface), but the drop in pressure, attributed to the creation of planar defects and decrepitation, is similar in both cases. Surprisingly, from the fifth cycle on, the absorption peaks shift towards higher pressures (Figs. 3B and 4). This behavior was interpreted in terms of a surface poisoning process due to residual oxygen and/or moisture present in the gas (let us recall that sample A was cycled with extra-purified hydrogen, whereas sample B was hydrided directly from the gas source). In Fig. 4 we see that sample A absorption peaks move gradually and monotonically towards lower pressures as activation proceeds. On the other hand, sample B absorption peaks show an initial decrease in absorption pressure, similar to that of sample A, that stops approximately at the fifth cycle and changes into a shift towards higher pressures.

The evolution of peak shape can be followed in Fig. 3. In the case of sample A (Fig. 3A) there are no significant changes in shape. In the case of sample B (Fig. 3B), the peaks transform, showing a transition that reflects two opposite trends: on one hand, the activation phenomena that improve kinetics and on the other hand, the poisoning effects that impair kinetics. On the fifth cycle a small shoulder can be seen on the high-pressure side of the peak. This shoulder develops in the following cycles,

and at the eighth cycle it becomes predominant. Further cycling accentuates this transformation, and at the tenth cycle, the initial low-pressure peak almost disappeared. Similar changes in peak shape due to surface poisoning were observed in the Mg–H_2 system [6].

The changes in capacity for sample B were similar to those of sample A. An initial decrease from 1.56 ± 0.08 to 1.34 ± 0.08 wt% was observed from the first to the second absorption. After that, capacity does not alter within experimental error, *i.e.* poisoning only affects kinetics during the first 10 cycles.

These observations agree with previous results [13–15] where the effect of different gas impurities on $LaNi_5$ was analyzed. In the case of O_2 and H_2O impurities, Sandrock and Goodell identified three different stages on the evolution of hydrogen absorption in $LaNi_5$: an initial decline in kinetics with no capacity loss that was characterized as a retardation effect, an intermediate recovery of kinetics attributed to the nucleation of nickel clusters on the surface, and a final decay with capacity loss due to lanthanum oxidation. The results shown here are consistent with the first stage described above.

5. Conclusions

The kinetic behavior of $LaNi_5$ hydriding and dehydriding during the first activation cycles was analyzed using PPAD measurements. In agreement with literature results, the most important changes were observed from the first to the second absorption cycles. In this case, the hydriding pressure falls from approximately 2000 to 800 kPa. However, around 62 cycles are needed to completely activate the material.

Additionally, the effects of different purity levels on the hydrogen used were studied. It has been found that poisoning effects change the shape of the absorption and desorption peaks hindering kinetics but without having a noticeable effect on capacity after only 10 absorption and desorption cycles.

References

[1] L. Schlapbach, A. Zuttel, Nature 414 (2001) 353–358.
[2] MRS Bull. 27 (2002) 675–716, special issue on Hydrogen Storage.
[3] M. Bououdina, D. Grant, G. Walker, Int. J. Hydrogen Energy 31 (2006) 177–182.
[4] U. Eberle, G. Arnold, R. von Helmolt, J. Power Sources 154 (2006) 456–460.
[5] G. Sandrock, S. Suda, L. Schlapbach, in: L. Schlapbach (Ed.), Hydrogen in Intermetallics Compounds II, Springer, Berlin, 1992, pp. 197–258.
[6] G. Urretavizcaya, V. Fuster, F.J. Castro, Rev. Sci. Instrum. 76 (2005) 073902.
[7] G. Sandrock, G. Thomas, Appl. Phys. A 72 (2001) 153–155.
[8] E.H. Kisi, C.E. Buckley, E.M. Gray, J. Alloys Compd. 185 (1992) 369–384.
[9] P. Selvam, B. Viswanathan, C.S. Swamy, V. Srinivasan, Int. J. Hydrogen Energy 16 (1991) 23–33.
[10] D. Khatamian, F.D. Manchester, in: F.D. Manchester (Ed.), Phase Diagrams of Binary Hydrogen Alloys, ASM International, OH, 2000, pp. 62–73.
[11] G.-H. Kim, S.-G. Lee, K.-Y. Lee, C.-H. Chun, J.-Y. Lee, Acta Metall. Mater. 43 (1995) 2233–2240.
[12] Y. Nakamura, E. Akiba, J. Alloys Compd. 308 (2000) 309–318.
[13] G.D. Sandrock, P.D. Goodell, J. Less-Common Met. 73 (1980) 161–168.
[14] P.D. Goodell, J. Less-Common Met. 89 (1983) 45–54.
[15] G.D. Sandrock, P.D. Goodell, J. Less-Common Met. 104 (1984) 159–173.